International Journal of Safety and Security Engineering
Vol. 15, No. 2, February, 2025, pp. 233-245
Journal homepage: http://iieta.org/journals/ijsse

Geophysical Investigations for the Characterisation of the Landslide Zone, Pungalapampa-Puninhuayco-Alao, Chimborazo, Ecuador

Dania Costales-Iglesias[1], María Jaya-Montalvo[1,2,3], Joselyne Solórzano[1,2*], Paúl Carrión-Mero[1,2]

[1] Facultad de Ingeniería en Ciencias de la Tierra, Escuela Superior Politécnica del Litoral (ESPOL), Campus Gustavo Galindo, km. 30.5 Vía Perimetral, Guayaquil 090902, Ecuador
[2] Centro de Investigación y Proyectos Aplicados a las Ciencias de la Tierra, Escuela Superior Politécnica del Litoral (ESPOL), Campus Gustavo Galindo, km. 30.5 Vía Perimetral, Guayaquil 090902, Ecuador
[3] Facultad de Ingeniería en Mecánica y Ciencias de la Producción, Escuela Superior Politécnica del Litoral (ESPOL), Campus Gustavo Galindo, km. 30.5 Vía Perimetral, Guayaquil 090902, Ecuador

Corresponding Author Email: josbasol@espol.edu.ec

https://doi.org/10.18280/ijsse.150204

Received: 6 November 2024
Revised: 24 January 2025
Accepted: 12 February 2025
Available online: 28 February 2025

Keywords:
electrical resistivity, transient electromagnetic method, stratigraphic profiles, landslides and hazards

ABSTRACT

Road construction involves filling and excavation procedures, leaving slopes susceptible to geological, hydrological and geomorphological factors, increasing the risk of instability and threatening road infrastructure and surrounding communities. The Chimborazo Province in Ecuador, due to its geographic location, diverse topography with structurally complex soil strata and variations in subsurface stratigraphy, requires detailed investigations focused on geophysics and in situ soil testing. This study assesses slope stability by correlating geophysical and soil tests to generate slope stability measurements. The applied methodology is based on the analysis of surface conditions, application of geophysical exploration, geotechnical characterisation, analysis and slope stability strategies. In the characterisation of the slope, three altered test pits were made where it was determined that there are metavolcanic materials, gravel and colluvial geologically. By correlating geophysical tests, it was determined that in the centre of the slope, the most critical apparent resistivity values (90-140Ω·m) correspond to colluvial deposits. For stability, it is proposed to terrace the slope surface with crown ditches at each level due to the presence of water holes and, in the most critical areas, to place reinforcement mesh over the vegetation. The existence of seepage zones on the slope was determined as a triggering factor for instability. These strategies serve as a basis for decision-makers in improving road connections and socioeconomic development in Andean rural communities.

1. INTRODUCTION

In many cases, landslides are due to increased and expanded settlements in dangerous areas of high vulnerability or inadequate land use due to a lack of planning [1]. Implementing techniques to reduce geological risks and vulnerability is essential to determine disaster prevention and mitigation strategies [2]. According to the World Meteorological Organization (WMO), between 1990 and 2015, landslides accounted for 10% of disasters and 12% of human deaths in Latin America [3].

In the Andean countries, landslides have been frequent due to their complex morphology, geographic location, and geodynamics, associated with the margin of the active tectonic plate and hydrometeorological phenomena, such as "La Niña" and "El Niño" also known as El Niño-Southern Oscillation (ENSO) [1]. For example, in Colombia, approximately 32,000 landslides have been recorded between 1900 and 2016, with rain being the most common triggering factor, at 90%. In other Andean countries, including Ecuador, increases in the frequency of landslides have been observed, with landslides being the leading cause of deaths from natural disasters [4].

Generally, the characterisation and identification of the boundary of a landslide is carried out by drilling (direct method), which is viable but expensive [5]. In contrast, geophysical applications represent non–non-destructive methods that offer significant advantages over conventional techniques [6]. These methods reduce the risk of contaminant dispersion, improve understanding of subsurface geometry, and enable cost reduction [7]. Geophysical methods are based on the interpretation of contrasts of specific physical properties of the subsoil (e.g., electrical resistivity) [8].

The choice of the appropriate geophysical method depends on the physical property to which it responds, which determines and limits the range of possible applications [9]. The most common research fields in geophysics focus on permafrost mapping [10], determining the thickness of sediments on slopes, and exploring landslides' depth and internal structures [11].

The success of geophysical methods depends on a contrast

of physical properties [12], the depth and resolution of interest [7], geophysical calibration using geological or geotechnical data [13], the signal-to-noise ratio, and the cost of the exploration campaign [14].

The contrasts identified could be local anomalies within the landslide caused by the rugged topography [15]. Geophysical methods have developed considerably over the last 20 years thanks to technological progress, the development of portable equipment, and the inclusion of new software in data processing, which allows obtaining 2D and 3D images of the subsoil [16].

Most landslide studies apply geophysical techniques to obtain accurate and reliable results of heterogeneous landslide structures [16, 17]. Currently, Electrical Resistivity Tomography (ERT) is the most widely used geophysical method, particularly in identifying water infiltration, which is one of the causes of the triggering or reactivation of ground movements [15]. Some investigations have applied the Transient Electromagnetic Method (TEM) or TDEM in landslides, for example, in the Langhe-Piemonte region (Italy), the combination of electrical methods with TDEM allowed to detect the geomorphological conditions of the slope [18].

Other authors, such as Schmutz et al. [19] offered the joint inversion of TDEM data and Direct Current (DC) soundings when applied to the Super Sauze earth flow (France). Furthermore, Li et al. [20] evaluated the advantage of TDEM in Sichuan Province (China) for detecting seepage pathway systems in debris landslides.

Ecuador is located at the interaction of the Nazca oceanic plate convergence, resulting in the uplift of the Andean mountains, active volcanism, geological faults, and a high probability of landslides occurring [21]. Landslides in this region occur due to the high elevations and steep slopes [22].

Significant population growth has been observed, creating the need to create new spaces for urban development, causing deforestation and using hillsides as construction land [22]. The most important landslides are: "La Josefina" (Azuay province) in March 1993, "Gulag-Marianza" (Azuay province) in March 2022, and the most recent one in Alausí (Chimborazo province) in March 2023 [23].

According to Hack, 75% of the tertiary network in the country is in a state of deterioration, 68% of the areas are located more than five hours away, and only 16% of the Agricultural Production Units (UPA) receive technical assistance for the development of their productive activities [24, 25]. These factors contribute to increasing the vulnerability of rural areas, negatively affecting their capacity to respond and assist in the face of natural disasters [26].

In the Chimborazo Province, landslides have forced the change of the route of several roads, such as Bravo-López et al. [27]. On March 26, 2023, a landslide occurred in Alausí (south of the Chimborazo province), a city with 42,823 inhabitants, representing 10.6% of the Chimborazo Province. The landslide caused 43 deaths, 1,034 victims, 163 homes affected, and 57 houses destroyed [28]. This study used topographic data collection and geological and geophysical prospecting tests such as ERT [27].

The slope under study is located 30 km from Riobamba, Chimborazo. On April 23, 2023, a landslide occurred due to heavy rainfall in the area and runoff from crops located on the crown of the slope, making it unstable and hindering mobility and access to the affected areas.

This research uses electrical and electromagnetic (EM) geophysical methods to characterise a landslide in the central Andean zone of Ecuador. Specifically, a combination of Vertical Electrical Soundings (VES), ERT, and TDEM is used. In addition, a sampling of altered soil from the landslide was carried out to correlate with geophysical data.

In this context, the research question arises: How does integrating VES, ERT, TDEM, and soil studies allow the characterisation of the landslide zone to contribute to decision–making and risk management? The study aims to evaluate the stability of the landslide located on the Pungalapampa–Puninhuayco–Alao Road (Chimborazo) by integrating ERT, TDEM, and geotechnical tests such as test pits for the formulation of slope support strategies.

2. MATERIALS AND METHODS

2.1 Study area

The study area is in the Chimborazo Province, a rural parish of Pungalá located approximately 30km from the city of Riobamba (capital of the province). The site is characterised by steep slopes ranging from 30-50°, inclined towards the Alao River micro-basin (Figure 1). The altitude varies from 2,680 to 4,440m above sea level [29].

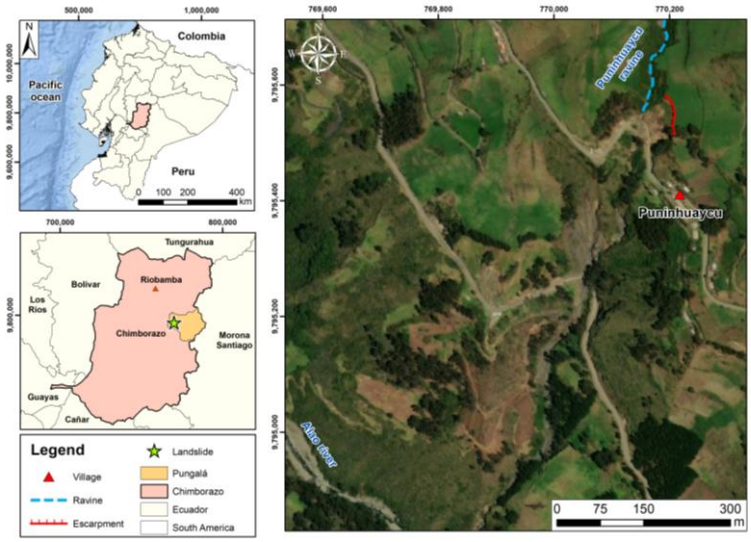

Figure 1. Location of the study area of the landslide scarp located in Puninhuayco, Chimborazo

The access roads to the communities are paved and gravelled, where the predominant products of the area are transported, such as potatoes, corn, beans, vegetables, barley, wheat, mellocos (andean tuber) and oca. The lithology of the site is composed of tuffs, clays, silts, andesites, agglomerates and basaltic rocks [30].

Historically, the population has developed its economic activities in agriculture and livestock. However, drought, primary production in small farms, poor road networks, lack of basic services, high levels of poverty, and lack of productive development have caused social problems such as migration [31]. The agricultural production generated in the sector serves to supply the markets of Riobamba. These activities are affected by mass movements, which mainly cover the main access routes, causing economic losses and human lives [30].

2.2 Methods

The research uses a quantitative approach based on a case study, using a combination of non-destructive geophysical techniques, laboratory tests, and natural stability analysis of the terrain, which allowed slope stability strategies to be generated (Figure 2).

During the field activities, a technical visit was conducted to assess the main damages, impacts, and existing risks, and the main characteristics of the slope slide were identified.

2.2.1 Phase I: Analysis of surface conditions

A visit was made to the study area to gather information, data and open interviews. Among the field activities, a preliminary assessment was made of the landslide that caused damage and risks. In addition, the topographic survey was carried out using the Leica FlexLine TS03 total station [32] to locate the coordinates that allowed the generation of plans and profiles using the AutoCAD software.

2.2.2 Phase II: Application of geophysical exploration and geotechnical characterisation

The local geology was surveyed, considering the sector's available base cartography and the main outcrops. This information, together with the results of Phase I, provided the input data for planning the geophysical exploration campaign, the geometry of the landslide and the structural conditions [33, 34].

A horizontal area with little vegetation was selected for the geophysical tests, interfering with the current, noise, and movement [35]. The electric current resistivity studies were carried out using the ABEM Terrameter SAS 1000 equipment, with the Schlumberger configuration, and the data was processed in the freely available software IPI2win (version 3.06.16), with an error percentage of less than 7%.

The tomograph, 21-output imaging cable and electrode cable junction were used for the ERT test with the Wenner configuration. Res2DInv software, version 4.10.3, was used for data processing. Regarding the TDEM, the equipment used was the Walktem 2, with a 40x40m transmitter coil. The test was performed at the top of the slope; the data was downloaded in GDB format (*.gdb) and processed in the licensed software Aarhus Spia, version 3.8, with layer modelling.

Additionally, soil sampling was carried out for the development of the following laboratory tests based on the American Society for Testing and Materials (ASTM) standard: i) specific weight, ii) shear strength, iii) simple compression, iv) particle size distribution and v) Atterberg limits. To extract samples, rectangular open pits of approximately 50-60cm depth were made on the slope [36]. It was decided to conduct three test pits in different slope areas, considering soil texture, topography, and other conditions.

In the specific weight essay of the soil, a representative fraction of the samples was selected to apply the cylinder method and estimate the volume by measuring the dimensions and determining its weight. The unconsolidated–undrained methodology was used for the shear strength test, where the friction angle and cohesion were obtained–fundamental parameters in the study of bearing capacity, slope stability, and lateral pressures, among other infrastructures [34]. A uniaxial compression test was also conducted by applying a compressive force between two plates to a cylinder until it failed, determining the material's stress [37].

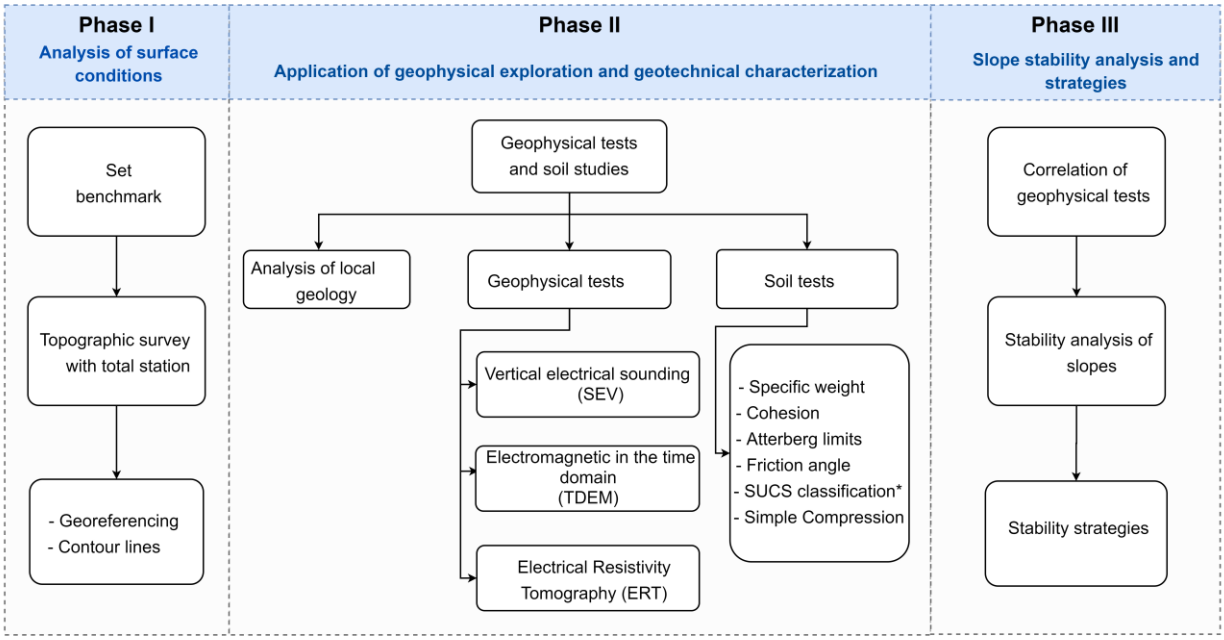

Figure 2. The methodological approach is divided into three phases of study
* Unified Soil Classification System (SUCS)

In the grain size analysis, the SUCS system was applied, which consists of observing and weighing the material from the sample that passes through the #200 sieve. When 50% of the sample's weight is retained on the mesh, it is defined as coarse material, and the second as fine material [38]. Then, the Casagrande Chart was used to determine the plastic limit, liquid limit, and plasticity index [36].

The geological correlation and geomechanical characterisation of the study area determined the properties of the materials and variations in the degree of saturation, resulting in a larger area and greater accuracy in the data [39].

Due to the limitations in accessibility for deep drilling and geotechnical testing, the distribution of materials in the subsoil at depths greater than 30m could be identified by correlating geophysical methods. Electrical resistivity measurements were associated with the mechanical properties of the materials, differentiating layers with different degrees of humidity and composition. Low resistivities indicate saturated or low compaction materials, so they can be correlated with soil instability, improving the understanding of geological conditions for stability analysis.

2.2.3 Phase III: Slope stability analysis and strategies

In the third phase, the correlation of topographic, geophysical, geomechanical data, and in situ observations was conducted for the slope stability analysis. In the first stage, topographic profiles were obtained along the extent of the slope using AutoCAD software. In the two-dimensional slope analysis study, SLIDE software (version 5.014) was used, applying the limit equilibrium method to calculate slope stability, which is widely used in geotechnics. The necessary data to analyse the slope in the software includes:

·Coordinates (x, y)
·Thicknesses of the strata
·Properties of the slope materials (specific weight, cohesion, and friction angle).

The soil properties were defined based on the geophysical and geological studies that have been carried out, which facilitate the determination of essential geotechnical parameters for the design of civil works [40].

The limit equilibrium method involves cuts made at the base of equilibrium, which must satisfy the equilibrium of forces and moments acting on individual blocks [41]. We must consider that the limit equilibrium method has certain limitations, as it does not consider deformations [42].

The calculation of the factor of safety (fs) was evaluated using two methods:

·The static method assumes that the acting and resisting forces are equal along the failure surface, equivalent to a value of 1.50.

·The pseudo-static method involves the acceleration in rock for the design earthquake (z), obtained from the seismic zoning map of Ecuador, resulting from the seismic hazard study (10% exceedance in 50 years) with a value of 1.05 [43].

The fs results were reviewed based on the Ecuadorian Construction Standard (NEC) to generate slope strategies, considering that the higher the coefficient, the greater the safety, ensuring stability [44, 45]. The strategies are crucial for conducting a detailed analysis and adapting to the specific conditions of the terrain and the project. The possible methods that can be used to correct slope instability can be divided into two groups: protection methods, which aim to prevent potential alteration phenomena from developing in the surface zone of the slope, and stabilisation or reinforcement methods, which involve actively intervening if these movements occur [46].

3. RESULTS

3.1 Analysis of surface conditions

In Figure 3 (a), the topography of the slope is presented, with a width of 40m and a total length of approximately 35m from the toe of the slope to the crest, forming an area of 1000m².

The slope is rotational, facing SW, and covering most of the roadway. The precipitation and high saturation from the crops at the crest of the slope create concentric and concave cracks in the direction of movement. In Figure 3 (b), the natural conditions of the landslide around the entire slope are evident.

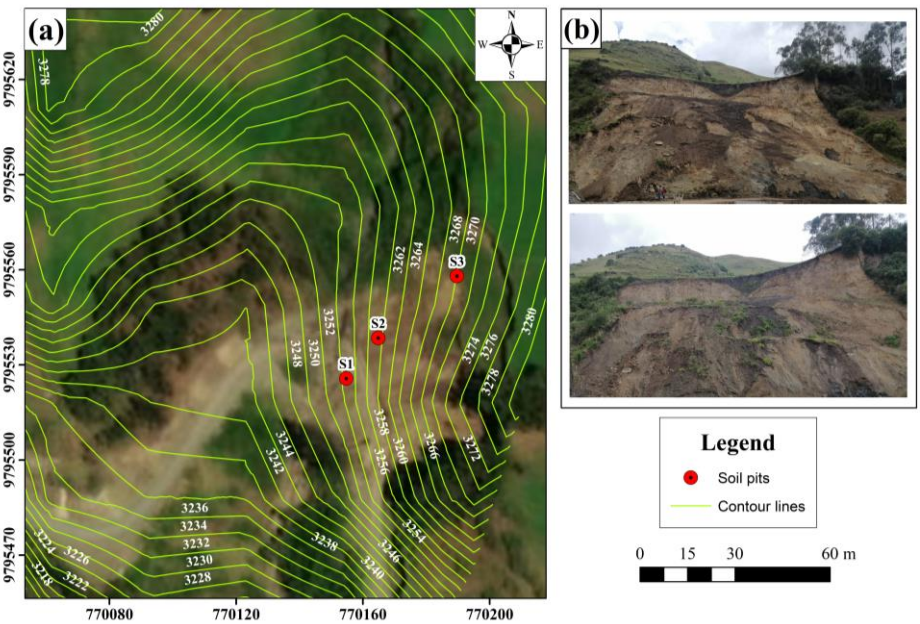

Figure 3. (a) Topographic map of the slope, (b) Photographs of the landslide that occurred on September 20, 2023

3.2 Geotechnical characterisation of the landslide

The geotechnical descriptions of the three test pits conducted at the base, centre, and crest of the slope, approximately 50cm deep, were based on in situ observations and laboratory test results. These materials were classified according to SUCS and NEC-SE-GC (Ecuadorian Construction Code, Geotechnics and Foundations) and are detailed as follows:

·Sample S1: moist grey silty sand, classified as SUCS type SM-silty sand.

·Sample S2: silty sand material with weathered igneous rock gravel, subjected to saturation conditions and classified as SUCS type SM.

·Sample S3: classified as SUCS type SC-clayey sand, considered suitable for cultivation due to its high nutrient levels, with fine particles predominating.

About the local geology, outcrops of volcanic tuffs, metavolcanic rocks, and colluvial deposits with predominant material of sands and gravels were identified. Below, Table 1 presents the results obtained from the laboratory tests of the test pits conducted at the toe (sample S1), centre (sample S2), and crest of the slope (sample S3).

Table 1. Results of geomechanical tests for obtaining physical properties

Tests		Sample S_1	Sample S_2	Sample S_3
Specific weight(g/cm³)		*2.65*	*2.55*	*2.72*
Moisture content (%)		*5.66*	*2.82*	*7.51*
Cohesion (kPa)		*25.20*	*25.10*	*35.77*
Atterberg limits	*Liquid limit (%)*	*0.30*	*0.27*	*33*
	Plastic limit (%)	*0.21*	*0.20*	*0.13*
	Plasticity index (%)	*0.09*	*0.07*	*20*
	Flow index	*0.22*	–	*0.10*
	Toughness index	*0.41*	–	*2.03*
	Consistency index	*1*	*1*	*1*
Friction angle (°)		*29.10*	*30.03*	*24.09*
Sigma (kg/cm²)		–	*0.58*	*0.65*
Qu max (kg/cm²)			*0.65*	
SUCS classification	D_{10}	*0.010*	*0.010*	*0.010*
	D_{30}	*0.200*	*0.210*	*0.08*
	D_{60}	*0.70*	*0.70*	*0.70*
	Cu	*70*	*70*	*70*
	Cc	*5.71*	*6.30*	*0.91*
	***SM:** Silty sands, sand–silt mixtures*			
	***SC:** Clayey sands, sand–clay mixtures*			

3.3 Results of applied geoelectric testing

In applying geophysical methods, six geoelectric tests were conducted throughout the study area (Figure 4). Three ERT tests with 8m spacing at the toe of the slope (total length of 160m), 2m in the transverse direction (total length of 40m), and 3m parallel at the top of the slope (total length of 60m). Two VES were conducted at AB/2 of 100m at the toe of the slope and AB/2 of 14.70m on the first terrace of the slope, with one TDEM test at the top of the slope.

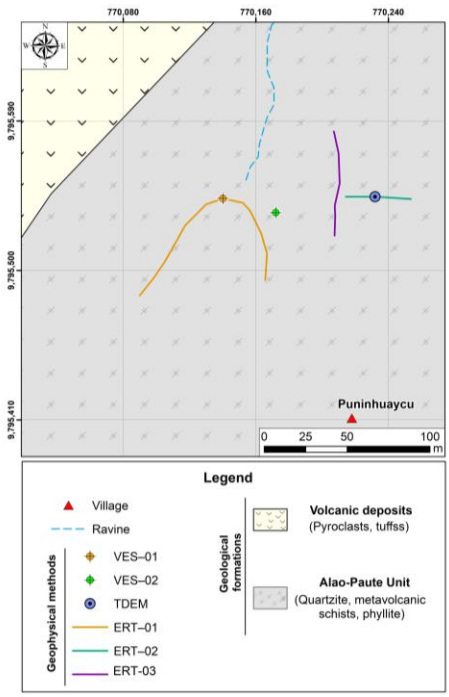

Figure 4. Geophysical test location map in the study area

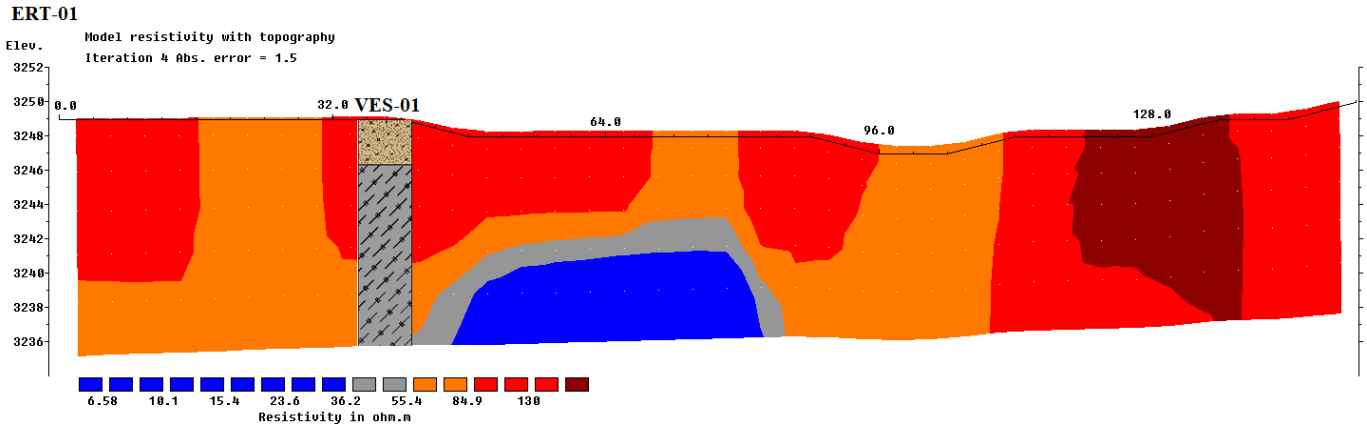

Figure 5. Correlation ERT-01 and VES-01 t the toe of the slope, with a length of 160m

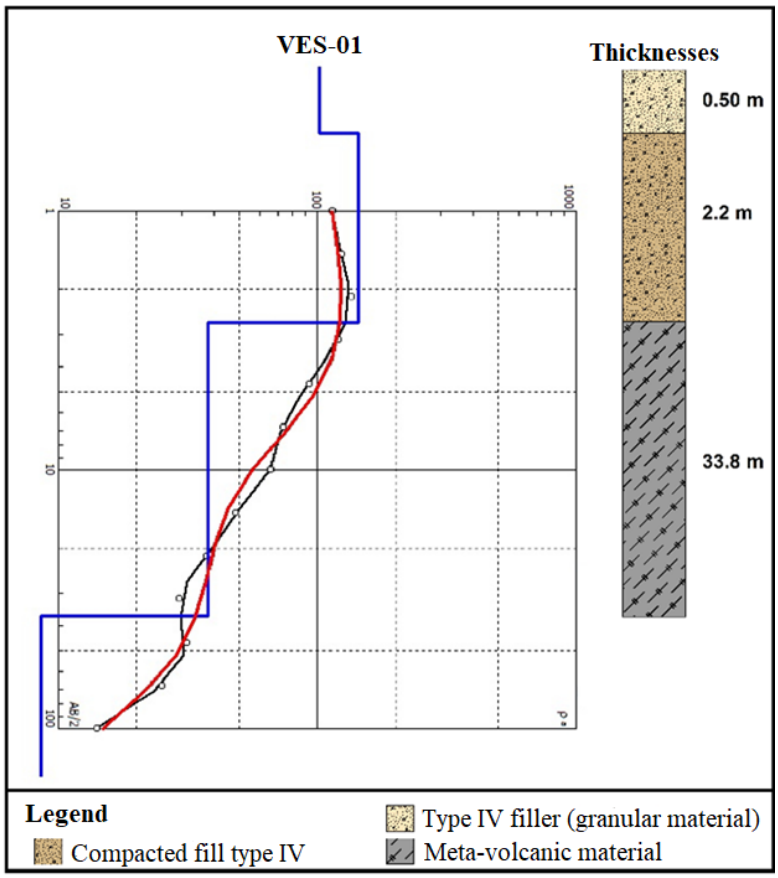

Figure 6. Electrical resistivity curve in the IPI2Win software with the representation of the stratigraphic column located at the toe of the slope

3.3.1 Electrical Resistivity Tomography 01

The ERT-01 reached a depth of 14m, with an electrical resistivity value ranging from 6.58 to 140Ω·m (Figure 5). The first 2m of the profile show high electrical resistivity values (>85 Ω·m), corresponding to the granular fill/ballast material type IV that has been placed as a base for the roadway.

To the west of the profile, below a depth of 2m, the high electrical resistivity values represent layers of slightly wet rock fragments. Along with the profile, the orange hues are associated with changes in the compaction and saturation of the material (60-85Ω·m). Low electrical resistivity values (26-60Ω·m) are observed in the central part of the profile, indicating the presence of wet meta–volcanic material, which implies a decrease in cohesion and the angle of internal friction, increasing the probability of slipping.

Meanwhile, the blue hue (<23 Ω·m) represents the saturated material in the drainage pipe installed to evacuate water from Puninhuayco Creek. In the VES-01 (Figure 6), a surface layer of 0.50 m was identified, corresponding to a type IV fill made of granular material (gravel or fragmented rocks). The underlying layer, 2.20m thick, shows higher electrical resistivity (144Ω·m), indicating the same type of material but more compacted due to lithostatic pressure. In the third layer, at a depth between 2.70 and 36.40m, the electrical resistivity drops to 38.10Ω·m, indicating a higher moisture content in the area's metavolcanic materials, decreasing the material's effective strength.

3.3.2 Electrical Resistivity Tomography 02 and 03

The ERT-02 conducted at the top of the slope, in a W–E direction, reached an approximate depth of 5m, while the ERT-03, in a N-S direction, reached a depth of 8m (Figure 7). In the ERT-02, four layers of material with different saturation levels were identified. In the initial part of the profile, electrical resistivity values ranging from 30-60Ω·m were recorded, with a thickness of 4m, corresponding to wet clays/silts.

At approximately 11m in length, a low electrical resistivity zone (20-30Ω·m) is observed due to the presence of material composed of saturated clays/silts. In the final part of the ERT-02, red colours represent areas of slightly moist colluvial deposits with intercalations of rock fragments (90-140Ω·m). In the correlation of ERT-02 with TDEM-01, the presence of slightly moist and loosely compacted colluvial soils is evident, with electrical resistivities ranging from 60–90Ω·m. These soils predominate along the profile, with certain intercalations that vary based on the degree of saturation and compaction.

Regarding ERT-03 (Figure 7), to the west of the profile, a material composed of wet and friable clays/silts is observed, as identified during the field survey, in the first 2m of depth. Below, a layer of slightly moist and loosely compacted colluvial soils is present, with electrical resistivities ranging from 60-90Ω·m and an approximate thickness of 1m. At depths greater than 4m, the electrical resistivities increase (>90Ω·m), corresponding to a layer of slightly moist colluvial deposits with intercalations of rock fragments.

On the eastern side, a thicker layer is shown with electrical resistivities between 30-60Ω·m, interpreted as wet clays/silts. In both profiles, it is evident how the degree of saturation varies with depth and the presence of fragments in specific areas. The identification of saturated zones has implications for slope stability due to its physical and mechanical characteristics since water in the pores can generate pressures that reduce the effective resistance of the material.

3.3.3 1D Geophysical tests conducted on the slope

The VES-02 carried out on the first terrace of the slope reached a depth of 2m, identifying two layers due to the small extension of the test (Figure 8). The first layer presents low electrical resistivities compared to the test carried out on the main road due to the change of material, where the value of 73.3Ω·m corresponds to slightly humid and poorly compacted colluvial soils, evidenced in the field survey.

While the underlying layer presents higher electrical resistivity values (345Ω·m) associated with colluvial soils with many dry rock fragments. In the upper part, the electromagnetic profile with an approximate penetration depth of 91m identified three layers of colluvial soils with different degrees of saturation (Figure 8). The first layer, with a thickness of 8.78m, has an electrical resistivity of 69.60Ω·m, corresponding to slightly moist and crumbly colluvial soil.

The second layer presents a slight variation in the electrical resistivity value (54.80Ω·m) due to the moisture content present in the area, classifying it as humid and poorly consolidated colluvial soils. From 60m, the electrical resistivity drops dramatically, with a value of 11.10Ω·m, relating it to a higher degree of saturation, corresponding to saturated colluvial deposits. These low electrical resistivity values represent saturated materials with variability in their geotechnical properties due to the deformation and weathering processes to which they have been exposed, giving rise to weak or weathered zones that act as preferred planes for landslides.

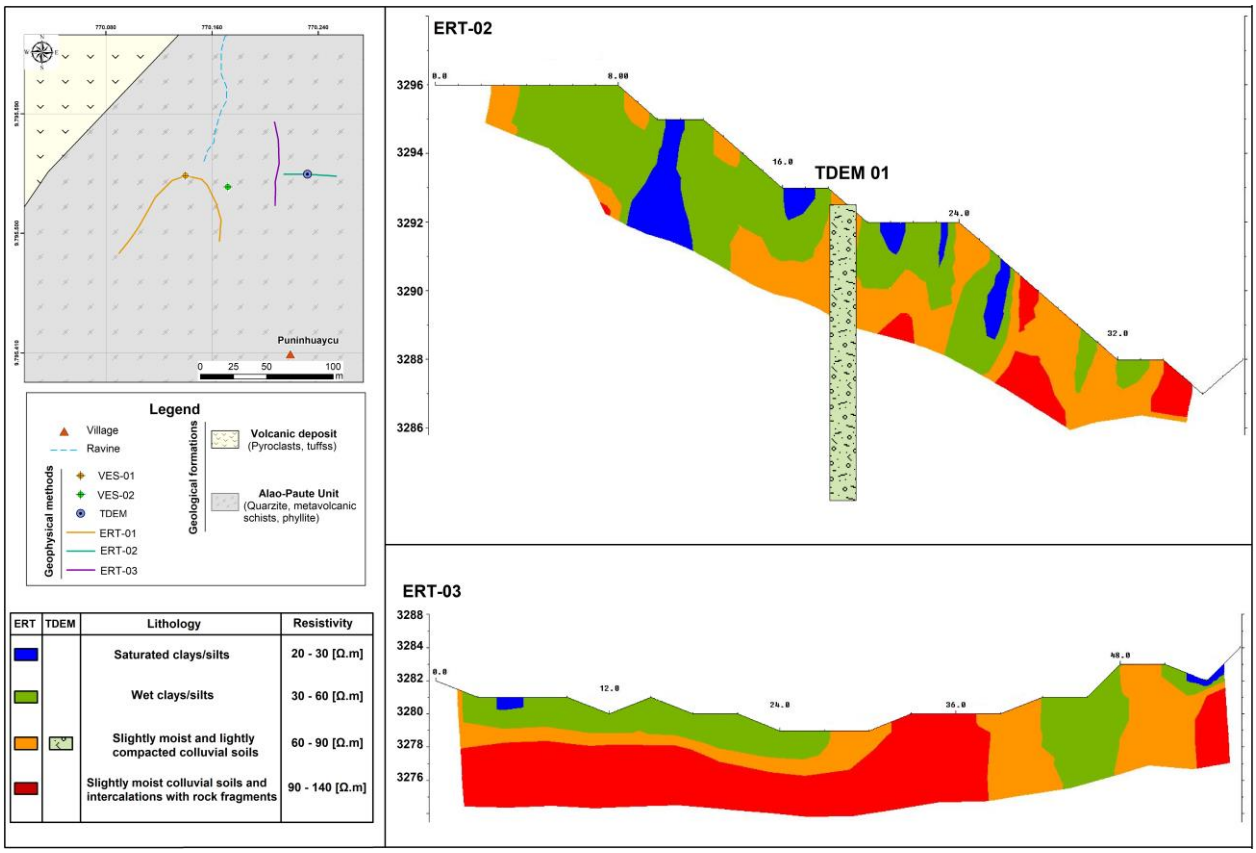

Figure 7. 2D geoelectric profiles conducted on the slope, ERT-02 located at the top of the slope, in a perpendicular direction with a length of 40m, correlated with TDEM-01, and ERT-03 in an E-W direction, with a length of 60m

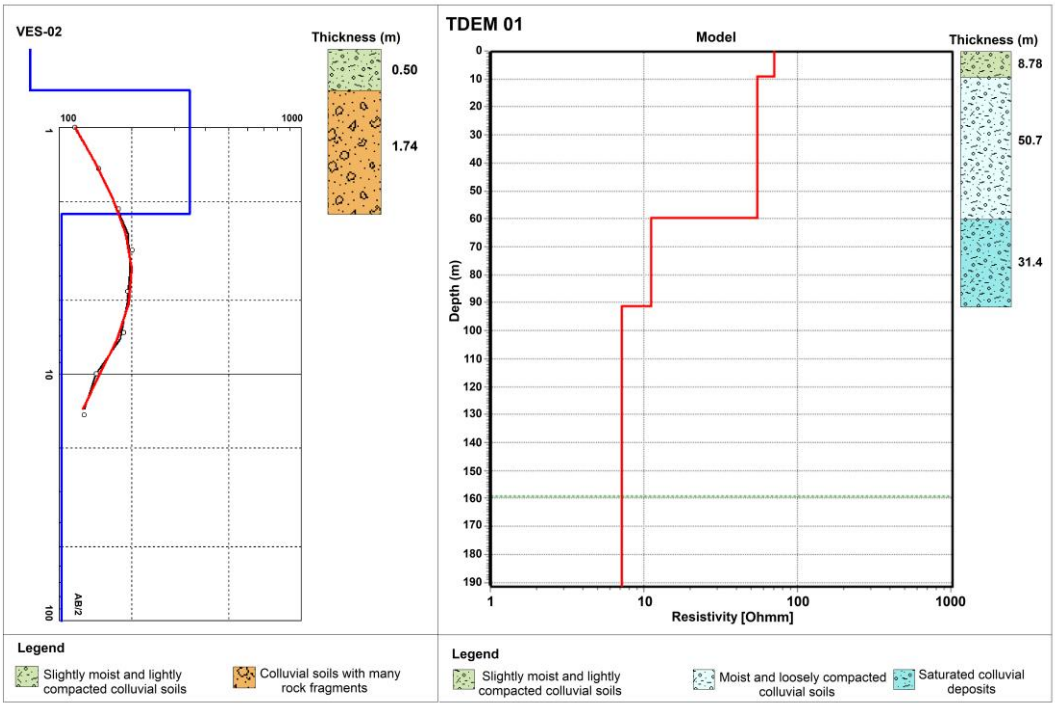

Figure 8. 1D tests performed on the slope, Vertical Electrical Sounding (VES-01) on the first terrace and TDEM-01 at the top of the slope

3.3.4 Correlation with geological conditions

Integrating ERT (Figure 7), VES (Figure 8), and TDEM (Figure 8) data strengthens the correlation between geophysical results and geological conditions. High electrical resistivity zones (>85Ω·m) identified in ERT and VES methods are consistent with compacted granular fill and dry colluvial deposits, while lower electrical resistivity values (<60Ω·m) correspond to saturated clays, silts, and weathered meta-volcanic materials. These findings are supported by direct field inspections, which revealed water accumulation and weak zones contributing to slope instability. The correlation provides a reliable framework for assessing slope stability and understanding the mechanisms driving landslides in the area.

3.4 Stability analysis

The NEC defines six soil profiles according to the shear wave velocity (Vs), soil moisture content (W), and other parameters (detailed in the Ecuadorian Standard for Construction Code Seismic Loads for Earthquake Resistant Design (NEC-SE-DS), part 1). To calculate the stability of the slope, computational tools were used where the surface of the landslide was analysed, using the limit equilibrium method, evaluating two conditions:

Static condition, analysing the slope without any support element, movement of masses or any other type of landslides to observe the behaviour of the slope in an initial state, obtaining an fs of 0.993 (Figure 9 (a)).

Pseudo-static conditions, the seismic hazard analysis in rock for a probability of exceedance of 10% in 50 years considered: soil type, seismic zone factor and soil amplification coefficient, resulting in an fs of 0.989 (Figure 9 (b)).

It was determined that the landslide presents concentric and concave cracks in the direction of the displacement, which produces fragmentation into blocks, and the most critical points were identified.

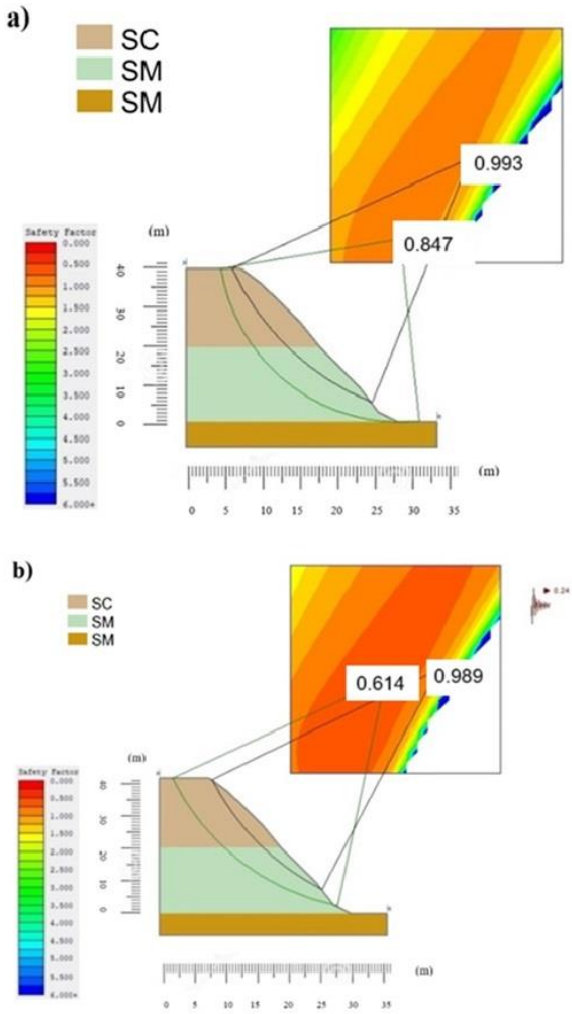

Figure 9. Calculation of the fs for the topographic profile a) static method b) pseudo-static method

3.4.1 Slope stability strategies

For the stability of an unstable slope, a surface treatment is necessary (Figure 10). One of the proposed strategies is to modify the geometry of the slope to reduce the forces that tend to the movement of masses and increase the resistance to shearing of the ground by increasing normal stresses [47]. As a result, the volume of unstable material will be reduced to prevent its mobilisation [48].

In addition, the profiling will begin from the top of the slope to control the runoff speed resulting from the crops found therein. Also, the top must be round to conserve moisture and plasticity characteristics, stimulate sufficient organic matter to cover the slope, and control erosion [49].

For the slope, the construction of three terraces will be contemplated, which will allow the elimination of irregularities and adaptation to the slopes [50], including intermediate berms, which are made in conjunction with the profiling, increasing the normal stresses and resistance at the base of the slope [51]. The function of berms is to facilitate the construction process, maintenance and intercept runoff [49].

Once the berms have been built, the crowning ditches will continue to control surface runoff and water erosion processes and avoid large volumes of infiltration [52]. The water coming from the crown of the slope is the result of irrigation from the crops, which infiltrate and accumulate, causing instability [46].

The geomembrane waterproofing is installed in areas where slow movements occur, and there is a need to control water infiltration. The proper placement of structures helps increase service life and reduce maintenance costs [53]. It should be installed over the excavated area, levelled and free of stones that could damage the geomembrane. Additionally, the pumping slopes should range between 4% and 6%, allowing for better drainage towards a concrete gutter at the base of the slope, which collects all the runoff water and directs it to an already constructed drainage system [54]. Finally, the entire slope will be covered with vegetation to prevent negative interaction between the civil works and the surrounding environment, thereby reducing the environmental impact [55]. It is easy to install because the maintenance costs are low compared to other processes [56].

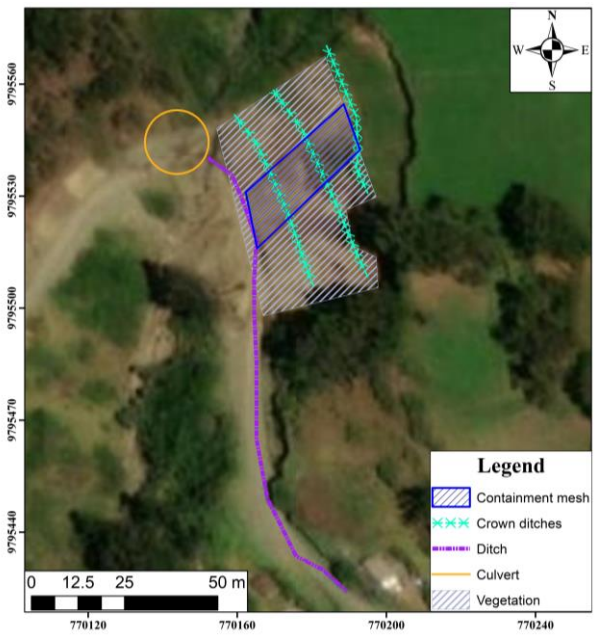

Figure 10. Location map with the proposal of stability strategies/measures based on in-situ conditions

4. DISCUSSION

This study provides a methodological approach that combines geophysical tests such as VES, ERT, and TDEM to obtain a 1D and 2D spatial view of the landslide. In addition to complementary studies of basic geomechanical tests on altered soil samples and slope stability analysis. This methodology considers several authors' recommendations on applying two or more geophysical methods to reduce ambiguity in interpretation [57, 54]. However, direct exploration methods such as drilling were not carried out due to their limited spatial reach (1D), ground conditions (loose material, presence of water springs), and safety considerations [55].

The proposed geophysical exploration strategy in the case study shows how the 1D geophysical surveys (Figure 7) exhibit a good correlation with the electrical resistivities obtained from the 2D geophysical methods on the interpreted slip surface (Figures 4-6), identifying colluvial soils with varying degrees of saturation, reaching depths of approximately 91m (Figure 7). Low electrical resistivities in the studied slope are associated with saturated clays/silts (<30Ω·m), critical stability implications, and unfavourable geological and geotechnical conditions. These saturated materials experience a decrease in their cohesion and internal friction angle due to increased water content, increasing the probability of slope failures, especially under additional loading conditions, such as heavy rains or earthquakes. Water in the materials increases their unit weight, which increases the gravitational forces acting on the slope, reducing the fs against sliding. Water accelerates weathering processes in meta-volcanic materials, making them more fragile and susceptible to failure. And in colluvial soils, saturation can break down finer particles (clayey/silty soils), further decreasing cohesion.

Slopes that have remained stable for a long time can eventually fail for several reasons due to their geology; for example, in the case study, it was determined through the SUCS classification that the material is SM at the base and centre of the slope and SC at the crown. This indicates that silty sands are characteristic of having high nutrient levels, as they have more porous spaces (clay soils have larger pores than sandy soils), which allows them to absorb and retain water more efficiently. Additionally, it tends to contract and expand with changes in moisture content, making it prone to erosion [58]. Slopes that have remained stable for a long time can eventually fail for several reasons, including their geology. For example, in the case study, it was determined through the SUCS classification that the material at the base and centre of the slope is SM (silty sands), while SC (clayey sands) was identified at the crown. This indicates that silty sands have high nutrient levels, as they contain more porous spaces (clayey soil has larger pores than sandy soil), allowing easy water absorption and retention. In addition, it tends to contract and expand with changes in moisture content, making it prone to erosion [59]. Silty-sandy soils also have high nutrient levels and drain slowly, which causes them to expand and retain moisture, making them weak soils [60].

The geotechnical methods used in the article allowed for calculating the fs using static and pseudo–static methods to determine stability conditions, identify unstable areas, and quantify landslide risks. In the modelled cases, a fs greater than 1 is not achieved, indicating that the slope could experience some mass displacement, considering the presence of water on the slope caused by pore pressure due to the

saturation level, which is the main factor to address. In addition to the suggested proposal, it was made to provide an immediate solution, even from an economic perspective.

Integrating geophysical and geomechanical data for the study of landslides and stability is key to obtaining complete data on the properties of materials. In areas where laboratory tests presented limitations due to their topography, for example, the combination of geophysical studies is complementary to expanding the analysis of the study area.

5. CONCLUSIONS

The slope characteristics were determined through the characterisation and correlation of geophysical and geotechnical tests. Geophysical methods, such as VES, ERT, and TDEM, were used to identify existing materials, including metavolcanic soils, clays/silts, and colluvial deposits.

The obtained results made it possible to determine that the slope is composed of SM and SC soils, which have high nutrient levels, making the soil fertile for the crops in the area. These soils are highly prone to erosion and drain slowly, which causes moisture retention and results in a weak soil structure.

The data obtained from the correlation between geotechnical and geophysical tests allowed for the determination of the material properties and variation in the saturation level of the slope, providing greater accuracy in the results as they cover a larger area.

The slope stability was designed under static and pseudo–static conditions based on limit equilibrium theory, determining the presence of concentric and concave cracks along the slope. The fs was more significant than one, depending on the slope's geometry and the geology that composes it. Some limitations affect the accuracy of the data obtained for the fs, which can lead to oversising in the design.

Finally, the strategy for stabilisation involves cutting the slope into terraces, including berms, to control the runoff speed caused by the crops located at the crown of the slope. This includes continuous crown trenches for each terrace and the installation of a geomembrane in areas with higher water infiltration. A gutter will be constructed at the base of the slope to collect water from the crown trenches, draining into the already constructed drainage system. Finally, the slope will be covered with vegetation to help prevent erosion and enhance stability.

The proposals were made from an economic and safety perspective, meaning the risk is imminent compared to any financial cost. However, failing to implement any intervention, despite the existing precedents, would leave the situation unresolved. These measures provide a provisional solution to stabilise the mass movement. The Pungalapampa community depends on planting and selling its products in Riobamba. Therefore, if a landslide were to occur on the slope, they would become isolated, as it is the only access route through the area. These situations are common in all Andean communities with similar conditions.

It is recommended that future investigations include complementary tests such as Standard Penetration Test (SPT) and seismic refraction surveys to further explore the characteristics of the study area in greater detail. Additionally, the design of retaining walls, anchors, and other civil works should be considered. It is also important to consider that Ecuador is highly seismic, so vulnerability maps should be developed, particularly for areas with surface runoff.

ACKNOWLEDGMENT

To the Master in Geotechnics (FICT-ESPOL) for all the knowledge imparted and academic excellence. The CIPAT-ESPOL provides logistical support, personnel, and geophysical equipment for field research. This work was supported by the research project "Registration of geological sites of interest in Ecuador for sustainable development strategies", Code CIPAT-004-2024 of the ESPOL Polytechnic University.

REFERENCES

[1] Martinod, J., Gérault, M., Husson, L., Regard, V. (2020). Widening of the Andes: An interplay between subduction dynamics and crustal wedge tectonics. Earth-Science Reviews, 204: 103170. https://doi.org/10.1016/j.earscirev.2020.103170

[2] Carrión-Mero, P., Montalván-Burbano, N., Morante-Carballo, F., Quesada-Román, A., Apolo-Masache, B. (2021). Worldwide research trends in landslide science. International Journal of Environmental Research and Public Health, 18(18): 9445. https://doi.org/10.3390/ijerph18189445

[3] Turner, A.K. (2018). Social and environmental impacts of landslides. Innovative Infrastructure Solutions, 3: 1-25. https://doi.org/10.1007/s41062-018-0175-y

[4] Miele, P., Di Napoli, M., Guerriero, L., Ramondini, M., Sellers, C., Annibali Corona, M., Di Martire, D. (2021). Landslide awareness system (Laws) to increase the resilience and safety of transport infrastructure: The case study of pan-American highway (Cuenca-Ecuador). Remote Sensing, 13(8): 1564. https://doi.org/10.3390/rs13081564

[5] Furuya, G., Katayama, T., Suemine, A., Kozato, T., Watanabe, T., Marui, H. (2013). Application of the newly frequency domain electromagnetic method survey in a landslide area. Landslide Science and Practice: Volume 2: Early Warning, Instrumentation and Monitoring, Springer, Berlin, Heidelberg, 169-175. https://doi.org/10.1007/978-3-642-31445-2_22

[6] Sai, V.V., Hemalatha, T., Ramesh, M.V. (2017). An affordable non-destructive method for monitoring soil parameters in large scale using electrical resistivity technique. In 2017 International Conference on Wireless Communications, Signal Processing and Networking (WiSPNET), Chennai, India, IEEE, pp. 755-761. https://doi.org/10.1109/WiSPNET.2017.8299862

[7] Alonso-Pandavenes, O., Bernal, D., Torrijo, F.J., Garzón-Roca, J. (2023). A comparative analysis for defining the sliding surface and internal structure in an active landslide using the HVSR passive geophysical technique in Pujilí (Cotopaxi), Ecuador. Land, 12(5): 961. https://doi.org/10.3390/land12050961

[8] Cappelli, F., Costantini, V., Consoli, D. (2021). The trap of climate change-induced “natural” disasters and inequality. Global Environmental Change, 70: 102329. https://doi.org/10.1016/j.gloenvcha.2021.102329

[9] Stewart, M.T. (1999). Geophysical investigations. In Seawater intrusion in coastal aquifers-Concepts, methods and practices. Dordrecht: Springer Netherlands. Springer, Dordrecht, pp. 9-50. https://doi.org/10.1007/978-94-017-2969-7_2

[10] Kurylyk, B.L., Walvoord, M.A. (2021). Permafrost hydrogeology. Arctic Hydrology, Permafrost and Ecosystems, Springer, Cham, 493-523. https://doi.org/10.1007/978-3-030-50930-9_17
[11] Leynaud, D., Sultan, N., Mienert, J. (2007). The role of sedimentation rate and permeability in the slope stability of the formerly glaciated Norwegian continental margin: The Storegga slide model. Landslides, 4: 297-309. https://doi.org/10.1007/s10346-007-0086-z
[12] Hack, R. (2000). Geophysics for slope stability. Surveys in Geophysics, 21(4): 423-448. https://doi.org/10.1023/A:1006797126800
[13] Hasan, M., Shang, Y., Jin, W., Akhter, G. (2020). An engineering site investigation using non-invasive geophysical approach. Environmental Earth Sciences, 79(11): 265. https://doi.org/10.1007/s12665-020-09013-3
[14] Jongmans, D., Garambois, S. (2007). Geophysical investigation of landslides: A review. Bulletin de la Société Géologique de France, 178(2): 101-112. https://doi.org/10.2113/gssgfbull.178.2.101
[15] Jongmans, D., Fiolleau, S., Bièvre, G. (2021). Geophysical monitoring of landslides: State-of-the art and recent advances. Understanding and Reducing Landslide Disaster Risk: Volume 3 Monitoring and Early Warning 5th, Springer, Cham, 75-84. https://doi.org/10.1007/978-3-030-60311-3_7
[16] Bortolozo, C.A., Mendes, T.S.G., Egas, H.M., Metodiev, D., de Moraes, M.V., de Andrade, M.R.M., Pryer, T., Ashby, B., Motta, M.F.B., Simões, S.J.C., Pampuch, L.A., Mendes, R.M., de Moraes, M.A.E. (2023). Enhancing landslide predictability: Validating geophysical surveys for soil moisture detection in 2D and 3D scenarios. Journal of South American Earth Sciences, 132: 104664. https://doi.org/10.1016/j.jsames.2023.104664
[17] Su, M., Cheng, K., Liu, Y., Xue, Y., Wang, P., Zhang, K., Li, C. (2021). Combining geophysical methods, drilling, and monitoring techniques to investigate carbonaceous shale landslides along a railway line: A case study on Jiheng Railway, China. Bulletin of Engineering Geology and The Environment, 80: 7493-7506. https://doi.org/10.1007/s10064-021-02365-5
[18] Nicolotti, G., Socco, L.V., Martinis, R., Godio, A., Sambuelli, L. (2003). Application and comparison of three tomographic techniques for detection of decay in trees. Journal of Arboriculture, 29(2): 66-78.
[19] Schmutz, M., Albouy, Y., Guérin, R., Maquaire, O., Vassal, J., Schott, J.J., Descloîtres, M. (2000). Joint electrical and time domain electromagnetism (TDEM) data inversion applied to the Super Sauze earthflow (France). Surveys in Geophysics, 21: 371-390. https://doi.org/10.1023/A:1006741024983
[20] Li, R., Hu, X., Xu, D., Liu, Y., Yu, N. (2020). Characterizing the 3D hydrogeological structure of a debris landslide using the transient electromagnetic method. Journal of Applied Geophysics, 175: 103991. https://doi.org/10.1016/j.jappgeo.2020.103991
[21] Orejuela, I.P., Toulkeridis, T. (2020). Evaluation of the susceptibility to landslides through diffuse logic and analytical hierarchy process (AHP) between Macas and Riobamba in Central Ecuador. In 2020 Seventh International Conference on eDemocracy & eGovernment (ICEDEG), Buenos Aires, Argentina, IEEE, pp. 201-207. https://doi.org/10.1109/ICEDEG48599.2020.9096879
[22] Wilcke, W., Valladarez, H., Stoyan, R., Yasin, S., Valarezo, C., Zech, W. (2003). Soil properties on a chronosequence of landslides in montane rain forest, Ecuador. Catena, 53(1): 79-95. https://doi.org/10.1016/S0341-8162(02)00196-0
[23] Harden, C. (2001). Sediment movement and catastrophic events: The 1993 rockslide at La Josefina, Ecuador. Physical Geography, 22(4): 305-320. https://doi.org/10.1080/02723646.2001.10642745
[24] Carrión-Mero, P., Solórzano, J., Cabrera, K.A., Vera-Muentes, B., Briones-Bitar, J., Morante-Carballo, F. (2023). Geotechnical characterization for territorial planning of a special economic zone at a university campus in Ecuador. Journal homepage: http://iieta. org/journals/ijdne, 18(4): 939-950. https://doi.org/10.18280/ijdne.180421
[25] Hack, R. (2000). Geophysics for slope stability. Surveys in Geophysics, 21(4): 423-448. https://doi.org/10.1023/A:1006797126800
[26] Briones-Bitar, J., Morante-Carballo, F., Chávez-Moncayo, M.Á., Blanco-Torrens, R., Carrión-Mero, P. (2022). Engineering solutions for the stabilisation of a hill located in an Urban Area. Case Study: Las Cabras Hill, Duran-Ecuador. International Journal of Sustainable Development & Planning, 17(3): 823-832. https://doi.org/10.18280/ijsdp.170312
[27] Bravo-López, E., Fernández Del Castillo, T., Sellers, C., Delgado-García, J. (2022). Landslide susceptibility mapping of landslides with artificial neural networks: Multi-Approach analysis of backpropagation algorithm applying the neuralnet package in Cuenca, Ecuador. Remote Sensing, 14(14): 3495. https://doi.org/10.3390/rs14143495
[28] Macías, L., Quiñonez-Macías, M., Toulkeridis, T., Pastor, J.L. (2024). Characterization and geophysical evaluation of the recent 2023 Alausí landslide in the northern Andes of Ecuador. Landslides, 21(3): 529-540. https://doi.org/10.1007/s10346-023-02185-6
[29] Thornthwaite, C.W. (1948). An approach toward a rational classification of climate. Geographical Review, 38(1): 55-94. https://doi.org/10.2307/210739
[30] Ilustre Municipio de Riobamba, Plan de Desarrollo y Ordenamiento-Gobierno Autónomo Descentralizado Municipal del Cantón Riobamba. https://gadmriobamba.gob.ec/index.php/la-municipalidad/la-alcaldia/plan-de-desarrollo-y-ordenamiento/pdot-2023-2035, accessed on Jan. 23, 2025.
[31] Kizil, U., Tisor, L. (2011). Evaluation of RTK-GPS and total station for applications in land surveying. Journal of Earth System Science, 120: 215-221. https://doi.org/10.1007/s12040-011-0044-y
[32] Leica Geosystems, Estaciones totales. https://leica-geosystems.com/es-es/, accessed on Jan. 23, 2025.
[33] Flamme, H.E., Krahenbuhl, R.A., Li, Y., Dugan, B., Shragge, J., Graber, A., Sirota, D., Wilson, G., Gonzales, E., Ticona, J., Minaya, A. (2022). Integrated geophysical investigation for understanding agriculturally induced landslides in southern Peru. Environmental Earth Sciences, 81(11): 309. https://doi.org/10.1007/s12665-022-10382-0
[34] Di Matteo, L. (2012). Liquid limit of low-to medium-

plasticity soils: Comparison between Casagrande cup and cone penetrometer test. Bulletin of Engineering Geology and The Environment, 71: 79-85. https://doi.org/10.1007/s10064-011-0412-5

[35] Baker, R., Garber, M. (1978). Theoretical analysis of the stability of slopes. Geotechnique, 28(4): 395-411. https://doi.org/10.1680/geot.1978.28.4.395

[36] Özer, M. (2009). Comparison of liquid limit values determined using the hard and soft base Casagrande apparatus and the cone penetrometer. Bulletin of Engineering Geology and The Environment, 68: 289-296. https://doi.org/10.1007/s10064-009-0191-4

[37] Khajevand, R. (2018). Geotechnical investigations for landslide hazard and risk analysis, a case study: The landslide in Kojour Region, North of Iran. Innovative Infrastructure Solutions, 3(1): 54. https://doi.org/10.1007/s41062-018-0160-5

[38] Pansu, M., Gautheyrou, J. (2006). Handbook of soil analysis. Berlin, Heidelberg: Springer Berlin Heidelberg. https://doi.org/10.1007/978-3-540-31211-6

[39] Anbalagan, R. (1992). Landslide hazard evaluation and zonation mapping in mountainous terrain. Engineering Geology, 32(4): 269-277. https://doi.org/10.1016/0013-7952(92)90053-2

[40] Solorzano, J., Morante-Carballo, F., Montalvan-Burbano, N., Briones-Bitar, J., Carrion-Mero, P. (2022). A systematic review of the relationship between geotechnics and disasters. Sustainability, 14(19): 12835. https://doi.org/10.3390/su141912835

[41] Deng, D.P., Li, L., Zhao, L.H. (2017). Limit equilibrium method (LEM) of slope stability and calculation of comprehensive factor of safety with double strength-reduction technique. Journal of Mountain Science, 14(11): 2311-2324. https://doi.org/10.1007/s11629-017-4537-2

[42] Mebrahtu, T.K., Heinze, T., Wohnlich, S., Alber, M. (2022). Slope stability analysis of deep-seated landslides using limit equilibrium and finite element methods in Debre Sina area, Ethiopia. Bulletin of Engineering Geology and The Environment, 81(10): 403. https://doi.org/10.1007/s10064-022-02906-6

[43] Kumar, N., Verma, A.K., Sardana, S., Sarkar, K., Singh, T.N. (2018). Comparative analysis of limit equilibrium and numerical methods for prediction of a landslide. Bulletin of Engineering Geology and the Environment, 77(2): 595-608. https://doi.org/10.1007/s10064-017-1183-4

[44] MIDUVI-Ministerio de Desarrollo Urbano y Vivienda, Norma Ecuatoriana de la Construcción. Guayaquil, Ecuador, 2015. https://www.habitatyvivienda.gob.ec/documentos-normativos-nec-norma-ecuatoriana-de-la-construccion/, accessed on Jan. 23, 2025.

[45] Arias-Valencia, D.C., Aristizábal-Arias, J.A. (2024). Análisis probabilístico de estabilidad de taludes con falla planar en la Comuna Universitaria de la ciudad de Manizales (Colombia). Información Tecnológica, 35(3): 1-10. http://dx.doi.org/10.4067/s0718-07642024000300001

[46] Popescu, M.E., Sasahara, K. (2009). Engineering measures for landslide disaster mitigation. Landslides-Disaster risk reduction, Springer, Berlin, Heidelberg, 609-631. https://doi.org/10.1007/978-3-540-69970-5_32

[47] Hamedifar, H., Bea, R.G., Pestana-Nascimento, J.M., Roe, E.M. (2014). Role of probabilistic methods in sustainable geotechnical slope stability analysis. Procedia Earth and Planetary Science, 9: 132-142. https://doi.org/10.1016/j.proeps.2014.06.009

[48] Carrión-Mero, P., Solórzano, J., Morante-Carballo, F., Chávez, M.Á., Burbano, N.M., Briones-Bitar, J. (2022). Technical closure of the humberto molina astudillo hospital and its implications for sustainability, zaruma-Ecuador. International Journal of Sustainable Development and Planning, 17(2): 363-373. https://doi.org/10.18280/ijsdp.170202

[49] Wu, W., Switala, B.M., Acharya, M.S., Tamagnini, R., Auer, M., Graf, F., te Kamp, L., Xiang, W. (2015). Effect of vegetation on stability of soil slopes: numerical aspect. Recent Advances in Modeling Landslides and Debris Flows, Springer, Cham, 163-177. https://doi.org/10.1007/978-3-319-11053-0_15

[50] Kim, J., Salgado, R., Lee, J. (2002). Stability analysis of complex soil slopes using limit analysis. Journal of Geotechnical and Geoenvironmental Engineering, 128(7): 546-557. https://doi.org/10.1061/(ASCE)1090-0241(2002)128:7(546)

[51] Camera, C., Apuani, T., Masetti, M. (2015). Modeling the stability of terraced slopes: An approach from Valtellina (Northern Italy). Environmental Earth Sciences, 74(1): 855-868. https://doi.org/10.1007/s12665-015-4089-0

[52] Andreu, V., Khuder, H., Mickovski, S.B., Spanos, I.A., Norris, J.E., Dorren, L., Nicoll, B.C., Achim, A., Rubio, J.L., Jouneau, L., Berger, F. (2008). Ecotechnological solutions for unstable slopes: Ground bio-and eco-engineering techniques and strategies. Slope Stability and Erosion Control: Ecotechnological Solutions. Springer, Dordrecht, 211-275. https://doi.org/10.1007/978-1-4020-6676-4_7

[53] Bussière, B. (2010). Acid mine drainage from abandoned mine sites: Problematic and reclamation approaches. In Advances in Environmental Geotechnics: Proceedings of the International Symposium on Geoenvironmental Engineering in Hangzhou, China, September 8-10, 2009. Springer Berlin Heidelberg, pp. 111-125. https://doi.org/10.1007/978-3-642-04460-1_6

[54] Kumar, N.V., Asadi, S.S., Chandra, D.S., Shivamanth, A., Kumar, G.P. (2021). Design and analysis of earth slopes using geosynthetics. In Proceedings of the Indian Geotechnical Conference 2019: IGC-2019. Springer Singapore, I: 719-729. https://doi.org/10.1007/978-981-33-6346-5_62

[55] Li, J., Wang, X., Jia, H., Liu, Y., Zhao, Y., Shi, C., Zhang, F., Wang, K. (2021). Assessing the soil moisture effects of planted vegetation on slope stability in shallow landslide-Prone areas. Journal of Soils and Sediments, 21(7): 2551-2565. https://doi.org/10.1007/s11368-021-02957-4

[56] Kumar, A., Sharma, R.K., Mehta, B.S. (2020). Slope stability analysis and mitigation measures for selected landslide sites along NH-205 in Himachal Pradesh, India. Journal of Earth System Science, 129(1): 135. https://doi.org/10.1007/s12040-020-01396-y

[57] Datta, M. (2010). Factors affecting slope stability of landfill covers. In Advances in Environmental Geotechnics: Proceedings of the International Symposium on Geoenvironmental Engineering in

Hangzhou, China. Springer Berlin Heidelberg, pp. 620-624. https://doi.org/10.1007/978-3-642-04460-1_65
[58] Yang, Q.W., Pei, X.J., Huang, R.Q. (2019). Impact of polymer mixtures on the stabilization and erosion control of silty sand slope. Journal of Mountain Science, 16(2): 470-485. https://doi.org/10.1007/s11629-018-4905-6
[59] Zakaria, M.T., Mohd Muztaza, N., Zabidi, H., Salleh, A.N., Mahmud, N., Rosli, F.N. (2022). Integrated analysis of geophysical approaches for slope failure characterisation. Environmental Earth Sciences, 81(10): 299. https://doi.org/10.1007/s12665-022-10410-z
[60] Islam, M.S., Begum, A., Hasan, M.M. (2021). Slope stability analysis of the Rangamati District using geotechnical and geochemical parameters. Natural Hazards, 108(2): 1659-1686. https://doi.org/10.1007/s11069-021-04750-5